AJNR

Morphologic and Hemodynamic Risk Factors in Ruptured Aneurysms Imaged before and after Rupture

A. Chien and J. Sayre

AJNR Am J Neuroradiol 2014, 35 (11) 2130-2135
doi: https://doi.org/10.3174/ajnr.A4016
http://www.ajnr.org/content/35/11/2130

Morphologic and Hemodynamic Risk Factors in Ruptured Aneurysms Imaged before and after Rupture

A. Chien and J. Sayre

ABSTRACT

BACKGROUND AND PURPOSE: Due to limited information about aneurysm natural history, choosing the appropriate management strategy for an unruptured aneurysm is challenging. By comparing unruptured and ruptured cases, studies have identified a variety of aneurysm morphologic and hemodynamic properties as risk factors for rupture. In this study, we investigated changes in 4 ruptured aneurysms before and after rupture and tested whether previously published risk factors identified a risk before rupture.

MATERIALS AND METHODS: A retrospective review of ruptured aneurysms based on the inclusion criteria of documenting angiographic images before and after rupture was performed. Such cases are extremely rare. To minimize hemodynamic influence due to location, we selected 4 cases at the posterior communicating artery. 3D morphologic and hemodynamic analyses were applied to examine qualitative and quantitative risk factors in aneurysms before and after rupture.

RESULTS: When we compared aneurysms before and after rupture, all increased in size. Volume, surface area, and morphology changed in both high and low wall shear stress areas. Aneurysm surface ratio, nonsphericity index, and pulsatility index were the only risk factors to consistently identify risk before and after aneurysm rupture for all aneurysms.

CONCLUSIONS: Although changes in shape and flow properties were found before and after aneurysm rupture, in this small study, we found that some risk factors were evident as early as 2 years before rupture.

ABBREVIATIONS: AASA = aneurysm surface area to sphere surface area ratio; AVSV = aneurysm volume to sphere volume ratio; NSI = nonsphericity index; PI = pulsatility index; SR = size ratio; WSS = wall shear stress

Due to limited information about aneurysm natural history, one of the biggest challenges in clinical aneurysm management is determining the risk of rupture for incidentally found aneurysms. Currently, size guidelines identified by the International Study of Unruptured Intracranial Aneurysms are the dominant criteria guiding treatment decisions.[1] Studies have suggested that the mechanisms underlying aneurysm rupture are multifactorial, and they have likewise identified different types of risk factors. For example, researchers have found that certain aneurysm shapes are risk factors that may associate aneurysm morphology with rupture.[2-4] By analyzing blood flow properties in groups of ruptured and unruptured aneurysms, reports have also shown that certain hemodynamic factors may play an important role in aneurysm rupture.[5-9] However, the morphologic and hemodynamic risk factors analyzed in these studies have generally been identified by analyzing ruptured aneurysms after rupture. Because clinical reports also suggest that aneurysms change due to rupture, how well these risk factors can actually help predict rupture has been controversial.[10-12]

In general, it is expected that the predictive ability of any aneurysm rupture risk factor will be higher as an aneurysm is closer to rupture. The fundamental rationale in aneurysm risk analysis based on comparing ruptured and unruptured aneurysm groups is that aneurysms that rupture have the same risk characteristics in the unruptured and ruptured states.[5-9,13] In that case, the results obtained by comparing ruptured with unruptured aneurysms can help assess the risk of rupture in as-yet-unruptured aneurysms. However, there are limited studies testing this hypothesis.

Received December 4, 2013; accepted after revision April 16, 2014.

From the Division of Interventional Neuroradiology (A.C.), David Geffen School of Medicine, and Department of Biostatistics (J.S.), School of Public Health, University of California, Los Angeles, Los Angeles, California.

This work was supported, in part, by a UCLA radiology exploratory research grant.

Paper previously presented in part at: Annual Meeting of the American Society of Neuroradiology, May 18–23, 2013; San Diego, California.

Please address correspondence to Aichi Chien, PhD, Division of Interventional Neuroradiology, David Geffen School of Medicine at UCLA, 10833 LeConte Ave, Box 951721, Los Angeles, CA 90095; e-mail: aichi@ucla.edu

Indicates open access to non-subscribers at www.ajnr.org

Indicates article with supplemental on-line table

http://dx.doi.org/10.3174/ajnr.A4016

In this study, we re-examined morphologic and hemodynamic risk factors that have been reported in the literature by using a unique dataset of aneurysms imaged in both their unruptured and ruptured states.[4,6-8,14-17] Our objective was to investigate morphology and flow properties of aneurysms before and after rupture and find whether previously identified risk factors were present in aneurysms before rupture. We sought to identify risk factors that consistently existed in ruptured aneurysms in both unruptured and ruptured states to guide early determination of aneurysm rupture risk.

MATERIALS AND METHODS

The study was approved by the institutional review board of the University of California, Los Angeles. A retrospective review of ruptured aneurysms with 3D images before and after rupture collected from the aneurysm database in the University of California, Los Angeles Medical Center was performed. Four aneurysms were included in this study. These cases were selected from the 729 ruptured aneurysms that were treated in our center from 1998 to 2012. The details of our case-selection method follow, to highlight the rarity of aneurysms with images before and after rupture. Among the ruptured aneurysms, anterior communicating artery, posterior communicating artery, and basilar artery with 203 (28%), 136 (19%), and 117 (16%) cases, respectively, were the 3 most common locations. Because aneurysm hemodynamic properties are affected by location, posterior communicating artery aneurysms (which had the most cases with before and after rupture images) were selected.[18] Six ruptured posterior communicating artery aneurysms had clinical images documenting aneurysms before and after rupture. The aneurysms were not treated because of advanced patient age. Only the 4 cases that had 3D images (either digital subtraction angiography or CT angiography) for both unruptured and ruptured states were included in this study. The 3D images recording the aneurysms before rupture were acquired in a range of 4 to 24 months prior to rupture. 3D images recording rupture were acquired within 24 hours of the rupture event.

The aneurysm 3D morphology before and after rupture was studied qualitatively and quantitatively on the basis of morphology risk factors previously found to correlate with rupture. Therefore, qualitative analysis was based on aneurysm lobulation (unilobular or multilobular).[16,17] Quantitative 3D morphology risk factors included aspect ratio, size ratio (SR), nonsphericity index (NSI), aneurysm volume ratio (AVSV), and aneurysm surface ratio (AASA) and were collected by using a previously developed automatic aneurysm geometry analysis tool.[4,19,20] Aspect ratio was defined as the ratio between aneurysm height and aneurysm neck (equation 1) proposed by Ujiie et al.[21] SR was defined as the ratio between aneurysm height and average parent artery diameter (equation 2),[15] and NSI was computed on the basis of the ratio of aneurysm volume and aneurysm surface area (equation 3) proposed by Raghavan et al.[3] AVSV was computed as the ratio of the aneurysm volume to the volume of a bounding sphere, defined by the longest distance between 2 points on the aneurysm (equation 4), as proposed by Chien et al.[4] AASA was calculated by comparing surface area in the same manner (equation 5). Previously reported thresholds for predicting rupture were used for each parameter[4,15,21]:

$$1)\quad \textit{Aneurysm aspect ratio} = \frac{(\text{aneurysm height})}{(\text{aneurysm neck})}$$

$$2)\quad \textit{Aneurysm size ratio} = SR = \frac{(\text{maximum aneurysm height})}{(\text{average parent artery diameter})}$$

$$3)\quad \textit{Aneurysm nonsphericity index} = NSI = 1 - (18\pi)^{1/3}\frac{(\text{aneurysm volume})^{2/3}}{(\text{aneurysm surface area})}$$

$$4)\quad \textit{Aneurysm volume ratio} = AVSV = \frac{(\text{aneurysm volume})}{(\text{bounding sphere volume})}$$

$$5)\quad \textit{Aneurysm surface ratio} = AASA = \frac{(\text{aneurysm surface area})}{(\text{bounding sphere surface area})}$$

Because several studies have found distinct hemodynamic properties in ruptured aneurysms, qualitative and quantitative hemodynamic risk factors previously reported as significant were reexamined for all aneurysms before and after rupture. A previously developed patient-specific hemodynamic simulation was applied to study aneurysmal flow before and after rupture. For all cases, a standard ICA flow profile acquired from a healthy subject with phase-contrast MR imaging was applied.[5,6,18,22] The qualitative hemodynamic risk factors analyzed included aneurysm inflow jet size, flow impingement size, and aneurysmal flow pattern, as proposed by Cebral et al.[5] Quantitative hemodynamic risk factors, including normalized wall shear stress (WSS), maximum aneurysm wall shear stress, and pulsatility index were analyzed.[8,15,22] On the basis of the indices proposed by Xiang et al,[15] normalized aneurysm wall shear stress was obtained by averaging wall shear stress over a cardiac cycle (equation 6), and maximum aneurysm wall shear stress was defined as maximum intra-aneurysmal WSS normalized by the average parent artery WSS (equation 7).[15] Pulsatility index (PI) is an index to analyze pulsatile flow changes at a specific region of an aneurysm. Using the flow rate collected at the aneurysm neck as proposed by Patti et al,[8] we calculated PI by finding the differences between the maximum and minimum flow rates divided by the mean flow rate in a cardiac cycle (equation 8). As with morphology parameters, reported risk values for distinguishing rupture and nonrupture with each index were used[8,15]:

$$6)\quad \textit{Normalized wall shear stress} = \frac{1}{T}\int_0^1 \left|\frac{\text{aneurysm WSS}}{\text{parent artery WSS}}\right| dt$$

where T is the duration of the cardiac cycle.

Summary of PcomA aneurysm cases before and after rupture

Case No.	Sex	Age (yr)	Side	Symptomatic/ Asymptomatic	Unruptured Size (mm)	Ruptured Size (mm)	Last Image before Rupture (mo)
1	F	75	Left	Asymptomatic	5.4	6.9	4
2	F	66	Left	Asymptomatic	11.6	11.9	12
3	F	72	Right	Asymptomatic	10.5	12.0	20
4	F	76	Left	Symptomatic	6.7	11.0	24

Note:—PcomA indicates posterior communicating artery.

7) *Maximum wall shear stress*

$$= \frac{\text{maximum aneurysm WSS}}{\text{average parent artery WSS}}$$

8) *Pulsatility index = PI*

$$= \frac{(\text{maximum flow rate}) - (\text{minimum flow rate})}{(\text{average flow rate})}$$

Statistical Analysis

To compare our results with other researchers' findings, descriptive statistics, including means, SDs, and confidence intervals, were calculated by using SPSS Statistics for Windows, Version 20.0. (IBM, Armonk, New York). Regression and correlation analysis, Mann-Whitney tests, and Student *t* tests with significance at the 5% level were used to compare risk factors in aneurysms before and after rupture.

RESULTS

Details of ruptured aneurysms included in this study are shown in the Table. Patients were all women, and the average age was 72.3 ± 4.5 years. Three of the aneurysms were incidentally detected, and 1 aneurysm was found due to mass effect. The On-line Table summarizes the results of morphologic and hemodynamic risk factors in aneurysms before and after rupture. With the exception of case 2, qualitative risk factors generally did not correctly identify high rupture risk before aneurysm rupture. All of the aneurysms exhibited morphology and size changes between the unruptured and ruptured time points (average growth, 1.90 ± 1.67 mm). 3D reconstructions of aneurysms before and after rupture based on 3D angiography are shown in Fig 1. Detailed analysis of 3D aneurysm curvature showed clearly that curvature changed between the unruptured and ruptured states (Fig 1*C*, -*D*, respectively). Aneurysm blebs were found in all aneurysms after rupture; however, only 2 cases (case 1 and case 2) had blebs present in the unruptured state.

3D quantitative comparison of aneurysm volume before and after rupture showed volume increases averaging 59.9 ± 25.7% and surface area increases averaging 31.8 ± 16.9%. Aspect ratio was, on the average, 1.69 ± 0.44 before aneurysm rupture and 1.96 ± 0.68 after rupture. SR was, on average, 2.68 ± 1.07 before and 3.27 ± 0.96 after rupture. Thus, a trend of increasing SR was found when comparing aneurysms before and after rupture. Seventy-five percent of aneurysms had SRs indicating rupture risk before rupture. NSI was, on average, 0.37 ± 0.09 and 0.30 ± 0.04 before and after rupture, respectively. All aneurysms were found to be at risk for rupture from assessment of NSI at both the unruptured and ruptured states. AVSV was, on average, 0.41 ± 0.10 and 0.46 ± 0.08 before and after rupture, respectively, showing a trend of AVSV increasing toward the risk threshold. AASA was, on average, 0.69 ± 0.07 and 0.67 ± 0.04 before and after rupture, respectively. All aneurysms were found to be at risk for rupture when assessing AASA at both the unruptured and ruptured states. There were no significant changes before and after rupture in aspect ratio, SR, NSI, AVSV, and AASA.

Figure 2 presents the results of hemodynamic analysis showing the WSS distributions and flow patterns in aneurysms before and after rupture at the end of systole. Using quantitative analysis, we found that normalized aneurysm wall shear stress was 1.85 ± 0.53 before rupture and 1.73 ± 0.26 after rupture, and in all of the cases, both before and after rupture, it did not indicate rupture risk. Maximum aneurysm wall shear stress was 2.35 ± 0.43 before rupture and 2.65 ± 0.48 after rupture. Maximum aneurysm wall shear stress indicated rupture risk both before and after rupture for only case 4. PI was, on average, 2.63 ± 0.63 before rupture and 2.57 ± 0.63 after rupture. Because in the previously published study of PI, risk was not identified on the basis of a particular numeric threshold but as trend, a residual analysis of regression by using previously reported trends by Patti et al[8] for PI was applied. For all cases, PI identified significant rupture risk before and after rupture. When we compared indices of normalized aneurysm wall shear stress, maximum aneurysm wall shear stress, and PI before and after rupture, none showed significant changes.

DISCUSSION

Previous studies of aneurysm rupture risk have analyzed ruptured aneurysms after rupture has occurred, primarily because image data for ruptured aneurysms before rupture are extremely rare. Whether we can use the knowledge gained by studying groups of ruptured and unruptured aneurysms to assess the risk of rupture remains an important question.

In this study, we found that NSI and AASA consistently indicated risk before rupture. Both NSI and AASA assess the irregularity of aneurysm morphology on the basis of the aneurysm 3D surface. NSI analyzes the ratio of volume and surface area in the aneurysm itself. AASA is computed solely on the basis of the surface area, comparing aneurysm surface area with the surface area of a minimal bounding sphere. Other morphologic indices, aspect ratio, SR, and AVSV, are not directly related to surface area and did not indicate rupture risk in the cases studied. Aspect ratio compares aneurysm height and neck, and SR compares aneurysm height and artery diameter. AVSV analyzes shape irregularity on the basis of volume ratio. We would expect similar results for indices similar to AVSV, such as undulation index, which is based on the volume ratio of the minimal convex volume around the aneurysm.[3] Although currently there is no defined biologic or pathophysiologic basis for these variables, our findings suggest

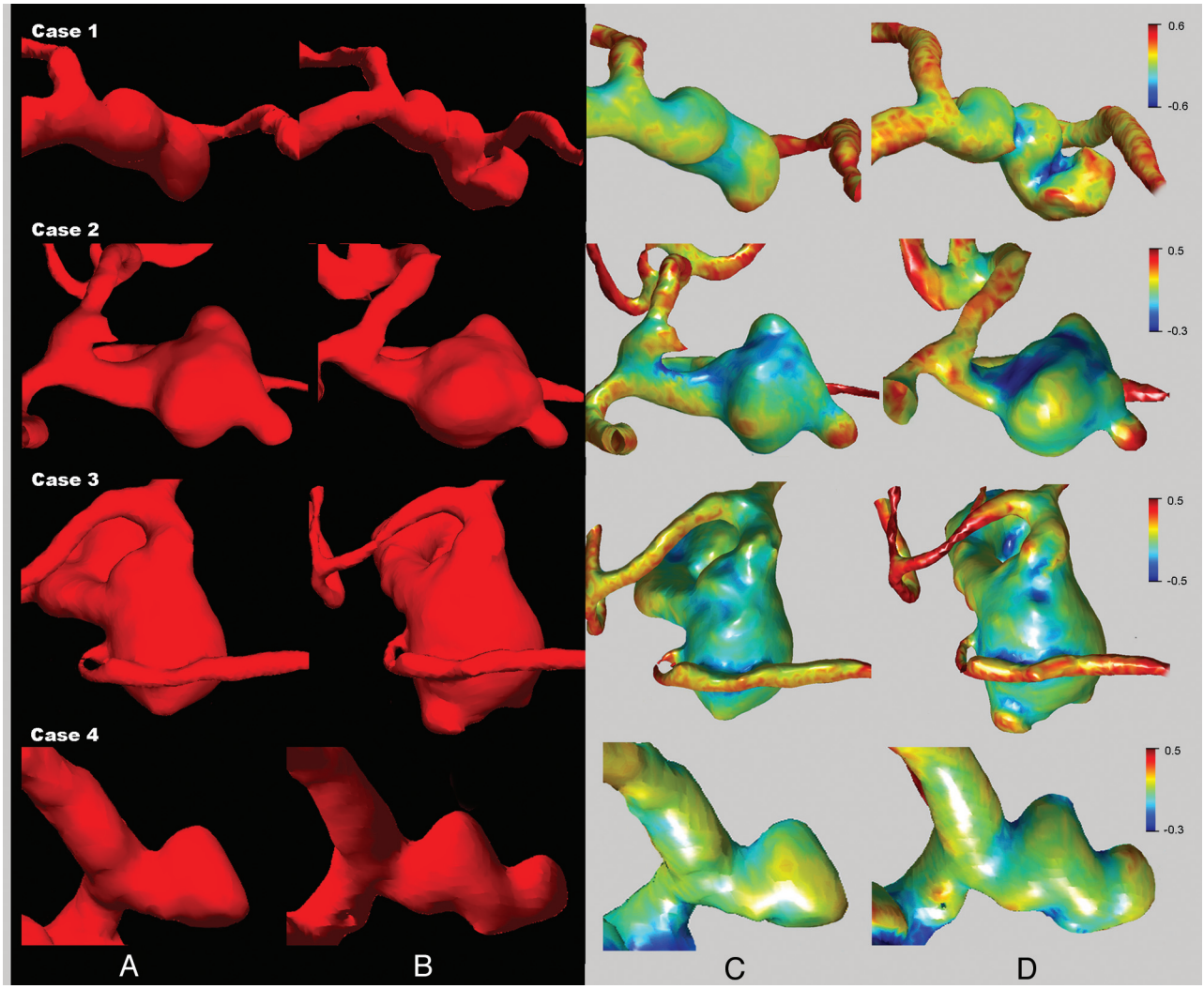

FIG 1. 3D reconstruction of aneurysm morphology before (*A*) and after (*B*) rupture. Quantitative morphology analysis of aneurysm curvature before (*C*) and after (*D*) rupture. High-curvature convex areas, such as blebs, are shown in red, with high-curvature concave areas shown in blue. Clear aneurysm morphology and curvature changes before and after rupture were found for all cases.

that surface-related indices such as NSI and AASA may be important morphologic bases to identify risk before rupture.

Our results showed that the WSS distribution changes before and after rupture in aneurysms (Fig 2*A*, -*B*). In the past, research analyzing unruptured aneurysms found that aneurysm growth was likely to occur at low WSS areas.[23] Our data showed that changes in aneurysm shape are not restricted to low WSS regions. As previously reported by Kono et al[24] in a study of a single posterior communicating artery aneurysm, we also found WSS changes before and after rupture. The present study of 4 ruptured aneurysms provides the first comparative data in individual aneurysms before and after rupture showing that WSS may change. As a result, while it appears that WSS, as the shear force on the aneurysm wall surface, may play an important role in eliciting a cellular response,[25,26] its value as a predictor of future aneurysm rupture was not supported by this study. Further studies with more cases are needed to understand the mechanism of WSS in the event of rupture and provide results with higher statistical power.

The other quantitative hemodynamic factor considered, the aneurysm pulsatility index, is a dynamic flow factor that examines the pulsatile flow properties within the aneurysm. As previously reported by Chien et al[6] and Baek et al,[27] aneurysm and vascular shape affect pulsatile flow properties at the aneurysm site. These effects are made especially clear when a single, standard flow profile is used for hemodynamic analysis of all cases, as is the standard method and was done in this research. We found that all cases in the present study, both before and after rupture, had high-risk PIs.[8] These results showed that before aneurysm rupture, all of these aneurysms already had pulsatile flow properties similar to those in previously studied ruptured aneurysms. Because PI is not correlated with morphologic parameters such as NSI or AASA, PI is an independent factor with potential value when combined to help assess rupture risk in unruptured aneurysms. Further study of the sensitivity of PI to different waveforms and heart rates is needed to better understand the relationship of PI to aneurysm rupture.

Limitations

Due to the risk of rupture, unruptured aneurysms are often treated before the rupture event occurs. In the present study, these aneurysms were followed to monitor changes and were not treated due to patient age.[1,28] Although we present only 4 cases, this is, to our

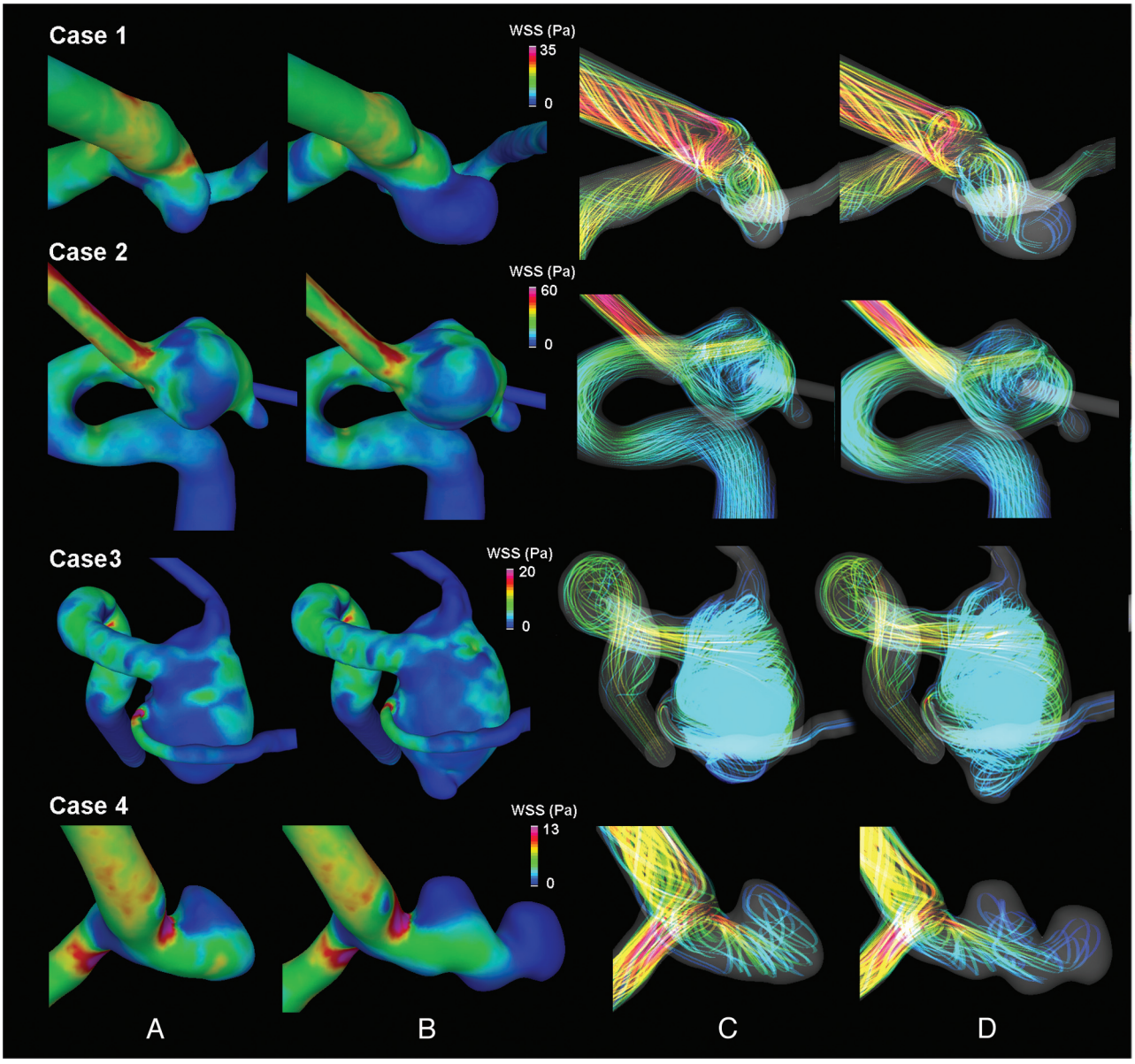

FIG 2. Results of hemodynamic analysis of systolic wall shear stress of ruptured aneurysms showed changes before (*A*) and after (*B*) rupture. The aneurysm flow pattern also changed before (*C*) and after (*D*) rupture.

knowledge, the largest number of cases analyzing morphology and hemodynamics before and after aneurysm rupture.[29] Because of software limitations, a few indices could not be included.[3,15] However, those analyzed represent most hemodynamic and morphologic indices previously associated with aneurysm rupture, and most excluded indices provide equivalent information to those included. To perform hemodynamic simulation, numeric models were made for aneurysms and arteries. These reconstruction procedures affected the outflow vessel geometry. Further improved algorithms to help reconstruct accurate vascular geometry for hemodynamic simulation are important to improve aneurysm risk analysis.

The main purpose of this study was to identify indices, among those previously found to relate to rupture, that do not change due to rupture. This study cannot distinguish imminent risk and permanent danger. How early aneurysms develop risk before rupture remains unclear. The statistical tests performed in this study were to allow comparisons with other research findings reported previously. The primary goal of statistical tests is not to provide information immediately applicable to clinical practice but to begin to evaluate the many computational indices developed during the past decade. While cases in which imaging was performed before and after rupture are likely to remain rare, larger longitudinal studies of growing aneurysms may provide insight into how various risk factors change during the growth process and allow more powerful statistical analysis. Additional work using follow-up data of unruptured aneurysms with matching size and location is needed to further understand whether the aneurysm changes associated with rupture may be distinct from changes associated with growth.

CONCLUSIONS

Changes in shape and flow properties were found by analyzing aneurysms before and after rupture. Through quantitative study

of morphologic and hemodynamic factors, this study indicates that while certain risk factors may primarily be evident after rupture (blebs, complex flow pattern, small inflow jet), other indicators of high aneurysm rupture risk may be found a considerable time before rupture. Specifically, the aneurysm surface ratio, nonsphericity index, and pulsatility index were consistent predictive risk factors. On the basis of the earliest available data for ruptured aneurysms before rupture, we found that by using these predictive risk factors, rupture risk could be detected as early as 2 years before rupture.

ACKNOWLEDGMENTS

The authors gratefully acknowledge Dr Fernando Viñuela in the UCLA Medical Center for providing the clinical ruptured aneurysm data base.

REFERENCES

1. Wiebers DO, Whisnant JP, Huston J 3rd, et al. **Unruptured intracranial aneurysms: natural history, clinical outcome, and risks of surgical and endovascular treatment.** *Lancet* 2003;362:103–10
2. Ujiie H, Tamano Y, Sasaki K, et al. **Is the aspect ratio a reliable index for predicting the rupture of a saccular aneurysm?** *Neurosurgery* 2001;48:495–502, discussion 502–03
3. Raghavan ML, Ma B, Harbaugh RE. **Quantified aneurysm shape and rupture risk.** *J Neurosurg* 2005;102:355–62
4. Chien A, Sayre J, Viñuela F. **Comparative morphological analysis of the geometry of ruptured and unruptured aneurysms.** *Neurosurgery* 2011;69:349–56
5. Cebral JR, Castro MA, Burgess JE, et al. **Characterization of cerebral aneurysms for assessing risk of rupture by using patient-specific computational hemodynamics models.** *AJNR Am J Neuroradiol* 2005;26:2550–59
6. Chien A, Sayre J, Viñuela F. **Quantitative comparison of the dynamic flow waveform changes in 12 ruptured and 29 unruptured ICA-ophthalmic artery aneurysms.** *Neuroradiology* 2013;55:313–20
7. Chien A, Tateshima S, Sayre J, et al. **Patient-specific hemodynamic analysis of small internal carotid artery-ophthalmic artery aneurysms.** *Surg Neurol* 2009;72:444–50, discussion 450
8. Patti J, Viñuela F, Chien A. **Distinct trends of pulsatility found at the necks of ruptured and unruptured aneurysms.** *J Neurointerv Surg* 2014;6:103–07
9. Shojima M, Oshima M, Takagi K, et al. **Magnitude and role of wall shear stress on cerebral aneurysm: computational fluid dynamic study of 20 middle cerebral artery aneurysms.** *Stroke* 2004;35:2500–05
10. Rahman M, Ogilvy CS, Zipfel GJ, et al. **Unruptured cerebral aneurysms do not shrink when they rupture: multicenter collaborative aneurysm study group.** *Neurosurgery* 2011;68:155–60, discussion 160–61
11. Wiebers DO, Whisnant JP, Sundt TM Jr, et al. **The significance of unruptured intracranial saccular aneurysms.** *J Neurosurg* 1987;66:23–29
12. Fargen KM, Mocco J. **Comment on: comparative morphological analysis of the geometry of ruptured and unruptured aneurysms.** *Neurosurgery* 2011;69:356
13. Takao H, Murayama Y, Otsuka S, et al. **Hemodynamic differences between unruptured and ruptured intracranial aneurysms during observation.** *Stroke* 2012;43:1436–39
14. Cebral JR, Mut F, Weir J, et al. **Association of hemodynamic characteristics and cerebral aneurysm rupture.** *AJNR Am J Neuroradiol* 2011;32:264–70
15. Xiang J, Natarajan SK, Tremmel M, et al. **Hemodynamic-morphologic discriminants for intracranial aneurysm rupture.** *Stroke* 2011;42:144–52
16. Hademenos GJ, Massoud TF, Turjman F, et al. **Anatomical and morphological factors correlating with rupture of intracranial aneurysms in patients referred for endovascular treatment.** *Neuroradiology* 1998;40:755–60
17. Beck J, Rohde S, el Beltagy M, et al. **Difference in configuration of ruptured and unruptured intracranial aneurysms determined by biplanar digital subtraction angiography.** *Acta Neurochir (Wien)* 2003;145:861–65, discussion 865
18. Chien A, Castro MA, Tateshima S, et al. **Quantitative hemodynamic analysis of brain aneurysms at different locations.** *AJNR Am J Neuroradiol* 2009;30:1507–12
19. Lederman C, Vese L, Chien A. **Registration for 3D morphological comparison of brain aneurysm growth.** In: *Advances in Visual Computing: Lecture Notes in Computer Science. Proceedings of the 7th International Symposium on Visual Computing*, Las Vegas, Nevada. September 2011;6938:396–403
20. Buades A, Chien A, Morel JM, et al. **Topology preserving linear filtering applied to medical imaging.** *SIAM Journal on Imaging Sciences* 2008;1:26–50
21. Ujiie H, Tachibana H, Hiramatsu O, et al. **Effects of size and shape (aspect ratio) on the hemodynamics of saccular aneurysms: a possible index for surgical treatment of intracranial aneurysms.** *Neurosurgery* 1999;45:119–29, discussion 129–30
22. Chien A, Tateshima S, Castro M, et al. **Patient-specific flow analysis of brain aneurysms at a single location: comparison of hemodynamic characteristics in small aneurysms.** *Med Biol Eng Comput* 2008;46:1113–20
23. Boussel L, Rayz V, McCulloch C, et al. **Aneurysm growth occurs at region of low wall shear stress: patient-specific correlation of hemodynamics and growth in a longitudinal study.** *Stroke* 2008;39:2997–3002
24. Kono K, Tomura N, Yoshimura R, et al. **Changes in wall shear stress magnitude after aneurysm rupture.** *Acta Neurochir (Wien)* 2013;155:1559–63
25. Malek AM, Alper SL, Izumo S. **Hemodynamic shear stress and its role in atherosclerosis.** *JAMA* 1999;282:2035–42
26. Reneman RS, Arts T, Hoeks AP. **Wall shear stress–an important determinant of endothelial cell function and structure–in the arterial system in vivo: discrepancies with theory.** *J Vasc Res* 2006;43:251–69
27. Baek H, Jayaraman MV, Karniadakis GE. **Wall shear stress and pressure distribution on aneurysms and infundibulae in the posterior communicating artery bifurcation.** *Ann Biomed Eng* 2009;37:2469–87
28. Bederson JB, Awad IA, Wiebers DO, et al. **Recommendations for the management of patients with unruptured intracranial aneurysms: a statement for healthcare professionals from the Stroke Council of the American Heart Association.** *Circulation* 2000;102:2300–08
29. Sforza DM, Putman CM, Scrivano E, et al. **Blood-flow characteristics in a terminal basilar tip aneurysm prior to its fatal rupture.** *AJNR Am J Neuroradiol* 2010;31:1127–31